Published in final edited form as:
Matrix Biol. 2008 March ; 27(2): 119–127.

The anion exchanger Ae2 is required for enamel maturation in mouse teeth

DM Lyaruu[1], **ALJJ Bronckers**[1], **L Mulder**[2], **P Mardones**[2], **JF Medina**[4], **S Kellokumpu**[5], **RPJ Oude Elferink**[3], and **V Everts**[1]

[1]*Dept. Oral Cell Biology, Universiteit van Amsterdam and Vrije Universiteit* [2]*Dept. Functional Anatomy, Academic Center for Dentistry Amsterdam (ACTA), Universiteit van Amsterdam and Vrije Universiteit* [3]*AMC Liver Center, Universiteit van Amsterdam, The Netherlands* [4]*Division of Gene Therapy and Hepatology, University Hospital/School of Medicine/CIMA, University of Navarra, and Ciberehd, Pamplona, Spain* [5]*Dept. Biochemistry, University of Oulu, Oulu, Finland*

Abstract

One of the mechanisms by which epithelial cells regulate intracellular pH is exchanging bicarbonate for Cl^-. We tested the hypothesis that in ameloblasts the anion exchanger-2 (Ae2) is involved in pH regulation during maturation stage amelogenesis. Quantitative X-ray microprobe mineral content analysis, scanning electron microscopy, histology, micro-computed tomography and Ae2 immuno-localisation analyses were applied to Ae2-deficient and wild-type mouse mandibles. Immuno-localisation of Ae2 in wild-type mouse incisors showed a very strong expression of Ae2 in the basolateral membranes of the maturation stage ameloblasts. Strikingly, zones of contiguous ameloblasts were found within the maturation stage in which Ae2 expression was extremely low as opposed to neighbouring cells. Maturation stage ameloblasts of the $Ae2_{a,b}^{-/-}$ mice failed to stain for Ae2 and showed progressive disorganisation as enamel development advanced. Maturation stage enamel of the $Ae2_{a,b}^{-/-}$ mice contained substantially less mineral and more protein than wild-type enamel as determined by quantitative X-ray microanalysis. Incisor enamel was more severely affected than molar enamel. Scanning electron microscopy revealed that the rod-inter-rod structures of the $Ae2_{a,b}^{-/-}$ mice incisor enamel were absent. Mineral content of dentine and bone of $Ae2_{a,b}^{-/-}$ mice was not significantly different from wild-type mice. The enamel from knockout mouse teeth wore down much faster than that from wild-type litter mates. Basolateral bicarbonate secretion via the anionic exchanger Ae2 is essential for mineral growth in the maturation stage enamel. The observed zonal expression of Ae2 in the maturation stage ameloblasts is in line with a model for cyclic proton secretion during maturation stage amelogenesis.

Keywords

Anion exchanger Ae2; enamel mineralisation; ameloblasts; knockout

Corresponding author: DM Lyaruu, Dept. Oral Cell Biology, ACTA, Universiteit van Amsterdam and Vrije Universiteit, v.d. Boechorststraat 7, 1081 BT Amsterdam, The Netherlands, Tel.: +31-20-4448666; Fax: +31-20-4448683 E-mail address: dm.Lyaruu@vumc.nl.

INTRODUCTION

Enamel is an epithelial product deposited by a unique, one cell-thick layer of tall cylindrical cells, the ameloblasts. These cells form the enamel in a two-step process. First, the ameloblasts secrete a provisional organic matrix, in which enamel crystals form. The enamel matrix consists mainly of amelogenins that initiate and stabilise the long thin enamel crystals. The initial enamel crystals are apatitic and grow preferentially in length within the organic matrix until almost the full enamel thickness is attained. This stage of enamel formation is called secretory amelogenesis. After completion of the secretory stage, the ameloblasts cease matrix deposition, shorten their cell bodies and after a short transitional stage, enter the maturation stage. Maturation stage triggers accelerated degradation of the extracellular matrix proteins mediated by serine proteases, such as kallikrein 4 (enamel matrix serine proteinase-1 or EMSP1) (Bartlett and Simmer, 1999) and is also accompanied by massive volumetric increase in enamel crystal size, mainly due to growth in width.

During formation of the hydroxyapatite crystals in the enamel compartment, protons are generated that need to be neutralised to maintain a physiological pH in order to drive the mineralisation process (Smith et al., 2005). The number of protons generated is dependent upon the phosphate precursor used and can vary between four and 14 moles of hydrogen per mole of apatite formed (Simmer and Fincham, 1995). The initial mineral deposited during the secretory stage of amelogenesis is thought to be mainly octacalcium phosphate (OCP) (Brown and Wallace, 1965; Brown et al., 1987). The relatively low rate of mineralisation during the secretory stage and the presence of large amounts of amelogenins with high buffering capacity in the enamel extracellular space are thought to be the mechanism responsible for neutralising the protons formed during OCP formation (Ryu et al., 1998; Simmer and Fincham, 1995). During the maturation stage, however, the situation is different: the rate of mineralisation is very high and the generation of protons is expected to be high as well while at the same time, the amelogenins that were responsible for buffering the extracellular compartment during the earlier secretory stage are being removed from the enamel compartment (Smith et al., 2005). If maturation ameloblasts are actively involved in proton buffering, one would expect that they secrete bicarbonate into the forming enamel. Indeed, the presence of cytoplasmic carbonic anhydrase type 2 (CA-II, which generates HCO_3^- and protons) in maturation stage ameloblasts supports this concept (Lin et al., 1994; Toyosawa et al., 1996). Assuming that bicarbonate is extruded into the forming enamel by the distal membranes, such concept requires that to maintain electro-neutrality protons are pumped away from the enamel compartment by a proton pump in the basolateral membranes (see for ion transporting epithelial cells: (Alper et al., 2002; van Adelsberg et al., 1993)). Remarkably however, maturation stage ameloblasts express a proton pump in the apical membrane (Lin et al., 1994), identical to the one found in the bone-resorbing osteoclasts (vacuolar H^+-ATPase, (Mulari et al., 2003)). The location of this vacuolar H^+-ATPase suggests paradoxically that the ameloblasts are secreting protons into the forming enamel instead of bicarbonate.

So far there is hardly any data pertaining to how ameloblasts regulate intracellular and extracellular pH during enamel formation. Smith et al. (Smith et al., 2006) reported the presence of carbonic anhydrase (CA-VI) in the enamel compartment that may function to buffer protons. These data suggest that bicarbonate exchange in ameloblasts may be crucial for the development of fully functional enamel. In addition, mice in which cystic fibrosis transmembrane conductance regulator (CFTR) responsible for chloride transport across epithelial membranes is mutated have severely softened enamel, suggesting that apical chloride secretion is also essential for amelogenesis (Sui et al., 2003).

Na^+-independent anion exchanger (Ae) is a ubiquitous gene family that mediates electroneutral exchange of Cl^- for HCO_3^- ions across cell membranes. Four different genes have been

identified in mammals so far: *Ae1, Ae2, Ae3 and Ae4*. Of these four genes, Ae2 is most ubiquitously expressed (Alper, 2002). The primary function of Ae2 is thought to be intracellular pH regulation, cell volume regulation and involvement in trans-epithelial hydroionic fluxes. In the mouse, five N-terminal isoforms of Ae2 have been recognised: *Ae2a, Ae2b1* and *Ae2b2, Ae2c1,* and *Ae2c2. Ae2a* is expressed in all tissues examined so far, while *Ae2b1* and *Ae2b2* are restricted to epithelial tissues and *Ae2c* is expressed mainly in the stomach (Alper et al., 2002).

Based on these reports we hypothesised that Ae2, localised in the membranes of maturation ameloblasts, (co)regulates the intracellular pH by the exchange of chloride for bicarbonate generated by carbonic anhydrase II. In the present study, we investigated the localisation of the Ae2 protein in ameloblasts and examined its function by analysis of the enamel of $Ae2_{a,b}^{-/-}$ knockout mice in which the Ae2a, Ae2b1 and Ae2b2 isoforms were disrupted (Medina et al., 2003).

RESULTS

The heterozygous animals were phenotypically indistinguishable from their wild-type litter mates. In addition, preliminary studies could not demonstrate any differences between the heterozygous and wild-type animals with respect to all the parameters reported in this study. Therefore, only the results pertaining to the knock-out and wild-type animals will be reported further in this study.

Gross morphology of erupted teeth

All molar and incisor teeth erupted into the oral cavity indicating that tooth eruption was not affected (Figs 1A–H). The enamel of the incisors in the $Ae2_{a,b}^{-/-}$ mice (Fig. 1C & D) lacked the typical yellow-orange pigmentation normally seen in the wild-type mice (Fig. 1A & B). At 40× magnification, the most profound effect of the $Ae2_{a,b}$ gene knockout was severe abrasion of the erupted teeth (Figs 1C & D, and G & H). Very little or no enamel at all could be observed in the $Ae2_{a,b}^{-/-}$incisors after eruption (cf. Figs 1A–B and Figs 1C–D). The μCT image (Fig. 1D) clearly showed that the incisor enamel was lost immediately after the tooth entered the oral cavity. The characteristic sharp cusp pattern seen in the $Ae2_{a,b}^{+/+}$ specimens (Fig. 1E & F) was lost in the $Ae2_{a,b}^{-/-}$ specimens (Fig. 1G & F), i.e., the molars were flattened due to severe abrasion (cf. Figs 1E–F & 1G–H). Although clearly abraded, an enamel layer was present in the erupted molars.

Light microscopy

Maturation stage ameloblasts in the $Ae2_{a,b}^{-/-}$ teeth were severely affected as observed by the cellular disorganisation and retention of organic matrix and cell fragments in the underlying enamel layer (cf. Figs 2A & 2B). The stratum intermedium and papillary cell layers adjacent to the ameloblast layer also appeared disorganised with extensive intercellular spaces (Fig. 2B). The structure of presecretory and secretory ameloblasts on the other hand, was not affected. Such lack of phenotypic changes was also true for the alveolar bone cells as well as the cells in the pulp chamber.

Mineral content (EPMA)

The positions of the analysed areas are shown in Figs 3A – D. Using back-scattered detector (BSD) electron optics, the enamel of $Ae2_{a,b}^{-/-}$ incisors appeared darker than the enamel of $Ae2_{a,b}^{+/+}$ specimens (cf. Figs 3A & B) suggesting a lower mineral content in the $Ae2_{a,b}^{-/-}$ enamel. The mineral elements calcium, phosphorus and magnesium account for most of the back-scattered electrons responsible for the BSD image acquisition. It should be noted here

that the images were acquired under exactly the same microscope parameters, a prerequisite for direct comparison of BSD images.

1) Incisor and molar enamel—The cumulative mineral content data for the incisors and molars are shown in Figs 4A and 4B, respectively. Both calcium and phosphorus contents in the $Ae2_{a,b}^{-/-}$ enamel specimens were significantly decreased in the incisor and molar when compared to the $Ae2_{a,b}^{+/+}$ specimens. This decrease in mineral content was however more pronounced in the $Ae2_{a,b}^{-/-}$ incisors than in the $Ae2_{a,b}^{-/-}$ molars (cf. Figs 4A & 4B). On the other hand, sulphur, a measure for amelogenin protein content, as well as magnesium were significantly higher in both incisor and molar enamel of the $Ae2_{a,b}^{-/-}$ mice.

2) Crown (enamel-related) and root (cementum-related) dentine in incisors—No significant differences in mineral content could be demonstrated between the $Ae2_{a,b}^{+/+}$ and $Ae2_{a,b}^{-/-}$ crown or root dentine (Figs 4C & 4D). It should be noted here that although no significant differences were found between the magnesium content in the root dentine of $Ae2_{a,b}^{+/+}$ and $Ae2_{a,b}^{-/-}$ animals, the magnesium content in root dentine of both the wild-type and knockout mice was always significantly higher than in the crown dentine.

3) Molar crown dentine—The only mineral parameter measured in the molars of the wild-type mice that significantly differed from the $Ae2_{a,b}^{-/-}$ mice was magnesium; i.e., in the $Ae2_{a,b}^{-/-}$ mice magnesium content in molar crown dentine was significantly higher than in the $Ae2_{a,b}^{+/+}$ molars (Fig. 4E).

4) Bone—Although magnesium content in the $Ae2_{a,b}^{-/-}$ alveolar bone specimens tended to be lower than in the $Ae2_{a,b}^{+/+}$ specimens, this difference was, not significant either for magnesium or for all other parameters measured (Fig. 4F).

Scanning electron microscopy

The characteristic rod-inter-rod structure seen in the $Ae2_{a,b}^{+/+}$ specimens (Figs 5A & B) was completely absent in the $Ae2_{a,b}^{-/-}$ specimens after acid etching (cf. Figs 5C & D). The surface of the $Ae2_{a,b}^{-/-}$ enamel appears amorphous with no evidence of enamel rod structure. No obvious differences in surface texture between the $Ae2_{a,b}^{+/+}$ and $Ae2_{a,b}^{-/-}$ specimens could be demonstrated in either bone or dentine.

Immunohistochemistry

The highest staining intensity for the Ae2 protein was found in the maturation stage ameloblasts of the $Ae2_{a,b}^{+/+}$ specimens and the staining was associated with the basolateral plasma membrane of the cells (Figs 6A & B). However, not all the maturation stage ameloblasts were equally intensely stained: each specimen contained some few contiguous cell populations with strikingly low staining intensity (Fig. 6C). The staining in the secretory ameloblasts was very low or absent and when present, it was mainly associated with the Golgi region. Erythrocytes were always intensely stained with this antibody due to the Ae1 that is highly expressed in these cells.

The staining pattern described above for the $Ae2_{a,b}^{+/+}$ specimens was completely absent in the $Ae2_{a,b}^{-/-}$ specimens (Fig. 6D). The only cells in $Ae2_{a,b}^{-/-}$ tissues that stained with the antibody to Ae2 were the erythrocytes in the blood vessel lumina (Fig. 6D, arrows).

Control sections of $Ae2_{a,b}^{+/+}$ tissue stained with non-immune antibodies were completely negative, including erythrocytes.

DISCUSSION

The data presented in this study demonstrate that a functional *Ae2* gene is necessary for proper enamel maturation in mouse teeth. The histological data suggest that the transitional-and-maturation stage ameloblasts were the cells most sensitive to loss of function of Ae2.

The Ae2 exchanger in the wild-type mice was localised in the basolateral membranes of the maturation ameloblasts similar to parietal cells in the gastric gland (Recalde et al., 2006) and in osteoclasts (Jansen, DC et al., 2007, personal communication). Both cell types secrete large amounts of protons, express cytoplasmic CA-II and have a proton pump in their apical membrane. Thus, our localisation data are consistent with the concept that the apical membranes of maturation ameloblasts may secrete protons and that basolateral membranes exchange bicarbonate for chloride to compensate for this proton flux. In line with this contention, Lin et al., (Lin et al., 1994) demonstrated the apical localisation of v-type H^+-ATPase in maturation stage ameloblasts. The lack of staining of maturation stage ameloblasts in *Ae2a,b*$^{-/-}$ mice confirmed that these cells do not express Ae2 and suggest that pH regulation in these cells is perturbed. Although weak immuno-staining for Ae2 was observed in the Golgi area of secretory ameloblasts in wild-type mice, no visible changes were noted in secretory stage amelogenesis in *Ae2a,b*$^{-/-}$ mice. In contrast to enamel, the other mineralising tissues, i.e., dentine and alveolar bone did not appear to have been markedly affected by Ae2 gene disruption, either morphologically or with respect to the degree of mineral deposition. So, defective mineralisation following a deletion of *Ae2* gene appears to be unique for the tooth enamel rather than for the other mineralising tissues.

The antibodies used in this study recognise Ae1 as well as all Ae2 isoforms. The positive staining of erythrocytes in *Ae2*$_{a,b}^{-/-}$ mice is attributed to Ae1 abundantly present in these cells. Since in Ae2$^{-/-}$ mice, the ameloblasts were completely negative for Ae2 immuno-staining, the data prove that *Ae2*$_{a,b}^{-/-}$ mice ameloblasts do not express Ae1 nor the Ae2 isoforms that were not knocked out (Ae2c1, c2). From this it may be inferred that normal ameloblasts only express Ae2a, and/or Ae2b1 and Ae2b2.

Enamel maturation is characterised by a dramatic decrease of organic matrix in the developing enamel accompanied by a massive increase in mineral content. During enamel maturation, the ameloblasts undergo a cyclic phenomenon, i.e., they are either smooth- or ruffle-ended at any given time. The pH of the enamel space under the smooth-ended ameloblasts is neutral (7.0 – 7.2) while that under the ruffle-ended ameloblasts is acidic (pH 5 – 6) (Sasaki et al., 1988), a condition that may drive proteolysis of the matrix. Ruffle-ended ameloblasts comprise about 80% of the maturation stage ameloblast population in the rat incisor. These ameloblasts are thought to be responsible for controlling the movement of calcium and other ions into the enamel space and thus control enamel crystal growth as well as enamel matrix resorption (Smith et al., 2005). It is interesting to note here that within the population of wild-type maturation ameloblasts some groups of cells stained weakly for Ae2 and we assume that these cells were less active and may correspond to the smooth-ended ameloblasts. The low mineral content and the presence of high organic matrix content (high sulphur content) in the maturation stage enamel reported here for the *Ae2*$_{a,b}^{-/-}$ mice suggest that in the absence of Ae2a,b mineral ion transport into the enamel space as well as protein resorptive capacity in maturation stage ameloblasts is seriously impaired.

The SEM data indicate that after acid etching, the characteristic enamel prism structure was lost in the *Ae2*$_{a,b}^{-/-}$ mice suggesting that disruption of the gene results in enamel crystal disorganisation and/or change in enamel mineral composition.

Significantly more mineral was found in the mature molar enamel than in the maturation stage enamel of the incisor of the *Ae2*$_{a,b}^{-/-}$ mice. This indicates that there are probably tissue

differences with respect to the function and/or expression of Ae2 in cells. Whether ameloblasts in the molar regulate pH differently or express different isoforms of Ae2 than in the incisor remains to be investigated.

Our working model for the possible function of Ae2 in enamel maturation is shown in Fig. 7. We assume that the ruffle-ended maturation stage ameloblasts maintain a low pH in the enamel layer to catalyse protein hydrolysis and/or drive the mineralisation process. To maintain this low pH, ameloblasts pump protons, generated by carbonic anhydrase II that is abundantly present in these cells, into the enamel space by the vacuolar H^+-ATPase associated with the ruffled border (Lin et al., 1994;Toyosawa et al., 1996). The Ae2 associated with the basolateral membranes of the ameloblasts exchanges extracellular Cl^- for intracellular HCO_3^-. The accumulated intracellular Cl^- is probably transported into the enamel compartment by the cystic fibrosis trans-membrane conductance regulator (CFTR, (Sui et al., 2003)). Conversely, in the smooth-ended ameloblasts Ae2 expression is severely down-regulated, suggesting that these cells secrete much less or no bicarbonate at the basolateral aspect and thus little or no protons into the enamel space. Indeed, more data is required to validate our model, in particular, regarding the pH gradient in the Ae2-deficient mice.

In conclusion, our data demonstrate that Ae2 is highly expressed in the basolateral membranes of maturation stage ameloblasts and is essential for the completion of mineral crystal growth in the maturation stage enamel in order to achieve its final hardness.

EXPERIMENTAL PROCEDURES

Animals and tissue processing

Mice carrying a targeted disruption of *Ae2* that prevents the expression of three Ae2 isoforms (Ae2a, Ae2b1, and Ae2b2) were generated as reported (Medina et al., 2003).

Mice, aged between six and twelve weeks were euthanised and the intact lower jaws dissected free of the adhering soft tissue and fixed in 4% formaldehyde in 0.1 M phosphate buffer, pH 7.4 overnight in the cold. After fixation, one hemi-mandible from each mouse was demineralised in 10% EDTA containing 0.8% formaldehyde, pH 7.4 for six weeks at room temperature on a shaker and then embedded in Technovit 8100 (Kultzer AG, Germany) according to manufacturers' instructions. The polymerised blocks were sectioned at 2 μm thickness and routinely stained with either toluidine blue or hematoxylin-eosin (HE). The other (non-decalcified) hemi-mandible was dehydrated in ascending alcohol series, embedded in methyl methacrylate (MMA) and further analysed for mineral content (see below). Five *Ae2*-deficient mice ($Ae2_{a,b}^{-/-}$) and four wild-type ($Ae2_{a,b}^{+/+}$) mice were analysed. In order to visualise the three-dimensional architecture of the mineralised tissues in the jaw, one representative MMA-embedded $Ae2_{a,b}^{+/+}$ and one $Ae2_{a,b}^{-/-}$ hemi-mandible were scanned at a resolution of 6μm voxels using μCT-40 high resolution scanner (Scanco Medical, AG, Bassersdorf, Switzerland) before preparation for the analysis of mineral content.

Immunohistochemistry

For the detection of Ae2 isoforms we used polyclonal rabbit antibodies raised against a synthetic peptide, identical to the 12 C-terminal-amino acids of the Ae2a protein as described by Holappa et al. (Holappa et al., 2001). These antibodies can recognise all Ae2 isoforms (Ae2a, Ae2b1, Ae2b2, and Ae2c) as well as the erythrocyte Ae1 (9 of the 12 C-terminal amino acid residues are identical to Ae2). The anti-sera were affinity purified and verified by Western blotting against the erythrocyte Ae1 and Ae2a protein.

Three $Ae2_{a,b}^{+/+}$ and $Ae2_{a,b}^{-/-}$ hemi-mandibles from adult mice were fixed overnight in 4% formaldehyde in 0.1 M phosphate buffer, pH 7.4, rinsed overnight in the same buffer and

decalcified as described above. The tissues were then washed overnight in 0.1 M phosphate buffer, pH 7.4, dehydrated in ascending alcohol series and routinely embedded in paraffin. Deparaffinized 5 μm-thick sections were stained with the affinity-purified anti-Ae2 antibodies at 1:600 dilution using the ABC-peroxidase methods (Elite Kit, Vectastain, Vector, Burlingame, CA, USA). Endogenous peroxidase was inactivated by incubation for 3 min in 3% hydrogen peroxide in phosphate buffered saline prior to immuno-staining. The immuno-staining was developed with DAB and counterstained with haematoxylin (Mayer). Normal rabbit IgG was used as negative control.

Electron probe microanalysis (EPMA)

The MMA-embedded jaw blocks were cut in a bucco-lingual plane approximately through the middle of the anterior cusps of the first molar. Mineral content was measured in the alveolar bone, incisors (enamel, crown and root dentine) and in molars (enamel, and dentine).

The trimmed tissue blocks were then re-embedded in a custom-made mould that fits into the specimen holder of the microprobe, polished, coated with graphite and then analysed for calcium, magnesium and phosphorus (mineralisation parameters) and also sulphur, a measure for methionine content. Methionine is the only sulphur-containing amino acid residue found in the amelogenins that comprise more than 90% of the enamel matrix proteins in the developing enamel (Termine et al., 1980). Survey micrographs were made using back-scattered detector (BSD) (Jeol Super Probe, JXA-8800) and used to define the areas to be analysed for mineral content. The incisor areas analysed were: enamel (3 measurement points), enamel-related dentine (3 measurement points), cementum-related dentine (3 measurement points) and alveolar bone (6 measurement points) (see Figs 3A & B for the positions of the analysis points). In the molar, six measurement points each were analysed in the enamel and enamel-related dentine as shown in Figs 3C & D. Cementum-related molar dentine was not analysed. The average of the analysed points in each tissue was regarded as one sampling point. Elements analysed were: calcium (expressed as CaO), phosphorus (expressed as P_2O_5), magnesium (expressed as MgO) and sulphur (expressed as SO_3).

EPMA analysis parameters

Microanalysis was performed under the following conditions: 15 KV accelerating voltage, 25 mA current and a spot size of 20 μm. Analysis times were 25 secs for calcium and phosphorus, 36 secs for magnesium, and 50 secs for sulphur.

Scanning Microscopy

After microanalysis, the graphite coating was removed from the surface of the blocks by gentle polishing and then the surface etched with 40% phosphoric acid solution for 30 secs, thoroughly washed with distilled water, dried, gold-palladium-coated and then observed in Jeol Super Probe scanning electron microscope.

Statistics

Values are presented as means and standard deviation (±SD). Significant differences were calculated using Student's *t*-test, and values were judged significant at $p \leq 0.05$ (two-sided).

Acknowledgements

This work was supported by NIH grant DE13508-06 (DL and AB) and by a grant from The Netherlands Organization for Scientific Research (NWO; program 912-02-073) to ROE. The authors wish to thank Dirk-Jan Bervoets and Paulien Holzmann for their technical assistance in tissue preparation and histology. Also, sincere thanks to Peter Brugman for performing the μCT analyses. The expertise, analytical support and hospitality of Wim Lustenhouwer, Wynanda Koot (Geotechnical Laboratory, Vrije Universiteit, Amsterdam), and Saskia Kars, at the Facilities for EPMA-analyses/SEM, Vrije Universiteit and NWO, The Netherlands Organization for Scientific Research, is highly appreciated.

References

Alper SL. Genetic diseases of acid-base transporters. Annu Rev Physiol 2002;64:899–923. [PubMed: 11826292]

Alper SL, Darman RB, Chernova MN, Dahl NK. The AE gene family of Cl/HCO_3 exchangers. J Nephrol 2002;15(Suppl 5):S41–S53. [PubMed: 12027221]

Bartlett JD, Simmer JP. Proteinases in developing dental enamel. Crit Rev Oral Biol Med 1999;10:425–441. [PubMed: 10634581]

Brown WE, Eidelman N, Tomazic B. Octacalcium phosphate as a precursor in biomineral formation. Adv Dent Res 1987;1:306–313. [PubMed: 3504181]

Brown WE, Wallace BM. Phase rule considerations and the solubility of tooth enamel. Ann N Y Acad Sci 1965;131:690–693. [PubMed: 5214656]

Holappa K, Suokas M, Soininen P, Kellokumpu S. Identification of the full-length AE2 (AE2a) isoform as the Golgi-associated anion exchanger in fibroblasts. J Histochem Cytochem 2001;49:259–269. [PubMed: 11156694]

Lin HM, Nakamura H, Noda T, Ozawa H. Localization of H(+)-ATPase and carbonic anhydrase II in ameloblasts at maturation. Calcif Tissue Int 1994;55:38–45. [PubMed: 7922788]

Medina JF, Recalde S, Prieto J, Lecanda J, Saez E, Funk CD, Vecino P, van Roon MA, Ottenhoff R, Bosma PJ, Bakker CT, Elferink RP. Anion exchanger 2 is essential for spermiogenesis in mice. Proc Natl Acad Sci U S A 2003;100:15847–15852. [PubMed: 14673081]

Mulari M, Vaaraniemi J, Vaananen HK. Intracellular membrane trafficking in bone resorbing osteoclasts. Microsc Res Tech 2003;61:496–503. [PubMed: 12879417]

Recalde S, Muruzabal F, Looije N, Kunne C, Burrell MA, Saez E, Martinez-Anso E, Salas JT, Mardones P, Prieto J, Medina JF, Elferink RP. Inefficient chronic activation of parietal cells in Ae2a,b(−/−) mice. Am J Pathol 2006;169:165–176. [PubMed: 16816370]

Ryu OH, Hu CC, Simmer JP. Biochemical characterization of recombinant mouse amelogenins: protein quantitation, proton absorption, and relative affinity for enamel crystals. Connect Tissue Res 1998;38:207–214. [PubMed: 11063028]

Sasaki T, Tadokoro K, Yanagisawa T, Higashi S, Garant PR. H^+-K^+-ATPase activity in the rat incisor enamel organ during enamel formation. Anat Rec 1988;221:823–833. [PubMed: 2847591]

Simmer JP, Fincham AG. Molecular mechanisms of dental enamel formation. Crit Rev Oral Biol Med 1995;6:84–108. [PubMed: 7548623]

Smith CE, Chong DL, Bartlett JD, Margolis HC. Mineral acquisition rates in developing enamel on maxillary and mandibular incisors of rats and mice: implications to extracellular acid loading as apatite crystals mature. J Bone Miner Res 2005;20:240–249. [PubMed: 15647818]

Smith CE, Nanci A, Moffatt P. Evidence by signal peptide trap technology for the expression of carbonic anhydrase 6 in rat incisor enamel organs. Eur J Oral Sci 2006;114(Suppl 1):147–153. [PubMed: 16674677]

Sui W, Boyd C, Wright JT. Altered pH regulation during enamel development in the cystic fibrosis mouse incisor. J Dent Res 2003;82:388–392. [PubMed: 12709507]

Termine JD, Belcourt AB, Miyamoto MS, Conn KM. Properties of dissociatively extracted fetal tooth matrix proteins. II Separation and purification of fetal bovine dentin phosphoprotein. J Biol Chem 1980;255:9769–9772. [PubMed: 7430100]

Toyosawa S, Ogawa Y, Inagaki T, Ijuhin N. Immunohistochemical localization of carbonic anhydrase isozyme II in rat incisor epithelial cells at various stages of amelogenesis. Cell Tissue Res 1996;285:217–225. [PubMed: 8766158]

van Adelsberg JS, Edwards JC, al Awqati Q. The apical Cl/HCO_3 exchanger of beta intercalated cells. J Biol Chem 1993;268:11283–11289. [PubMed: 8496183]

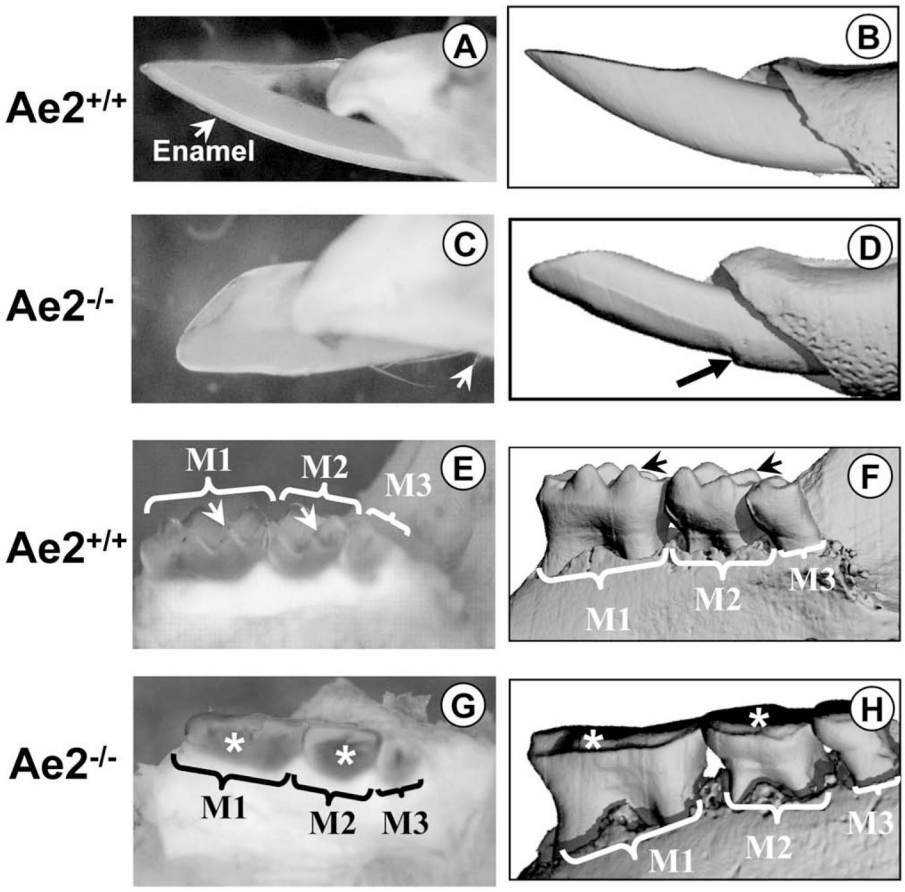

Figure 1A – H.

Fig. 1A is a macro-photograph of an erupted $Ae2_{a,b}{}^{+/+}$ incisor and Fig. 1B the μCT image of the same tooth. In Fig. 1A, the enamel can be clearly seen. Fig. 1C is a macro-photograph of an $Ae2_{a,b}{}^{-/-}$ incisor. Note that there is virtually no enamel present, only some remnants (white arrows). The corresponding μCT image of the same tooth is shown in Fig. 1D. The black arrow shows the eroded enamel just before it enters the oral cavity. The morphology of the $Ae2_{a,b}{}^{+/+}$ molars is shown in Figs 1E (macro-photograph) and 1F (μCT), respectively. The cusps of all molars (M1= first, M2= second and M3= third maxillary molars) are sharp (arrows) and are not eroded. The molars from the $Ae2_{a,b}{}^{-/-}$ specimen (Fig. 1G, macro-photograph and Fig. 1H, the corresponding μCT image of the same tooth) are severely eroded (asterisks).

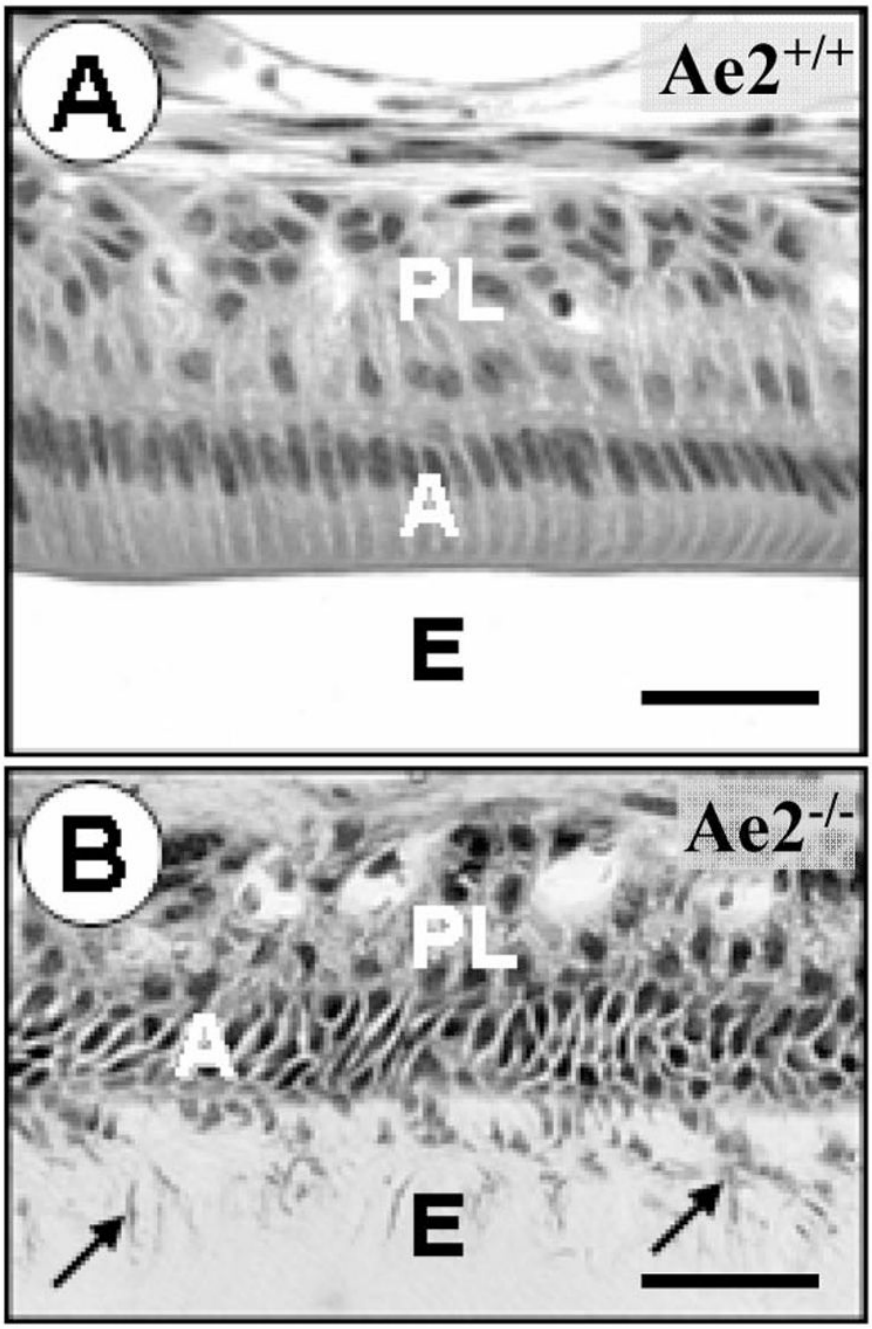

Figure 2A–B.

Fig. 2A is a micrograph of the maturation stage of a demineralised $Ae2_{a,b}^{+/+}$ incisor. The ameloblasts (A) as well as the papillary layer (PL) cells appear normal. The space originally occupied by enamel (E) does not stain because it is empty due to dissolution of the mineral during tissue processing for histology. Fig. 2B was taken of a comparable $Ae2_{a,b}^{-/-}$ specimen. The ameloblasts (A) are disorganised and cellular fragments can be seen in the enamel space (E, arrows). Note that the enamel space stains due to the presence of residual enamel matrix proteins. (haematoxylin-eosin stained; bars=25μm).

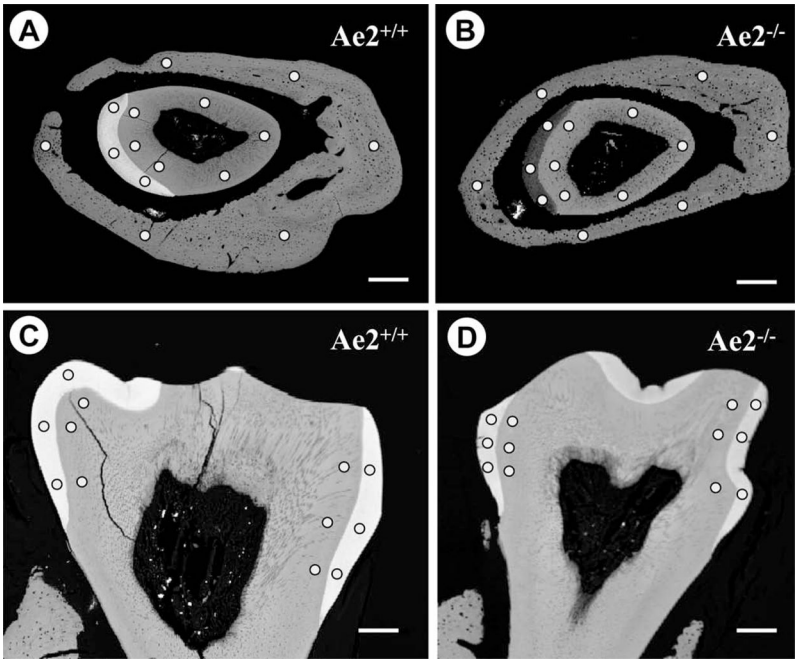

Figure 3A–B.

Low power back-scattered detector (BSD) micrographs and electron microprobe analysis areas: Fig. 3A is a BSD image of an $Ae2_{a,b}^{+/+}$ specimen cut through the maturation stage incisor enamel and that from the $Ae2_{a,b}^{-/-}$ specimen is shown in Fig. 3B. The low contrast in the $Ae2_{a,b}^{-/-}$ enamel compared to the $Ae2_{a,b}^{+/+}$ specimen indicates low level of mineralisation. Fig. 3C is of an $Ae2_{a,b}^{+/+}$ first molar and Fig. 3D of an $Ae2_{a,b}^{-/-}$ specimen. Note that the difference in electron density between the $Ae2_{a,b}^{+/+}$ (Fig. 3C) and $Ae2_{a,b}^{-/-}$ molar enamel (Fig. 3D) is less pronounced than that seen in the incisors (cf. Fig. 3A & B above). All the images were acquired under identical microscope parameters. The areas analysed for mineral content in enamel, dentine and bone are shown by dots. (Bars=300μm).

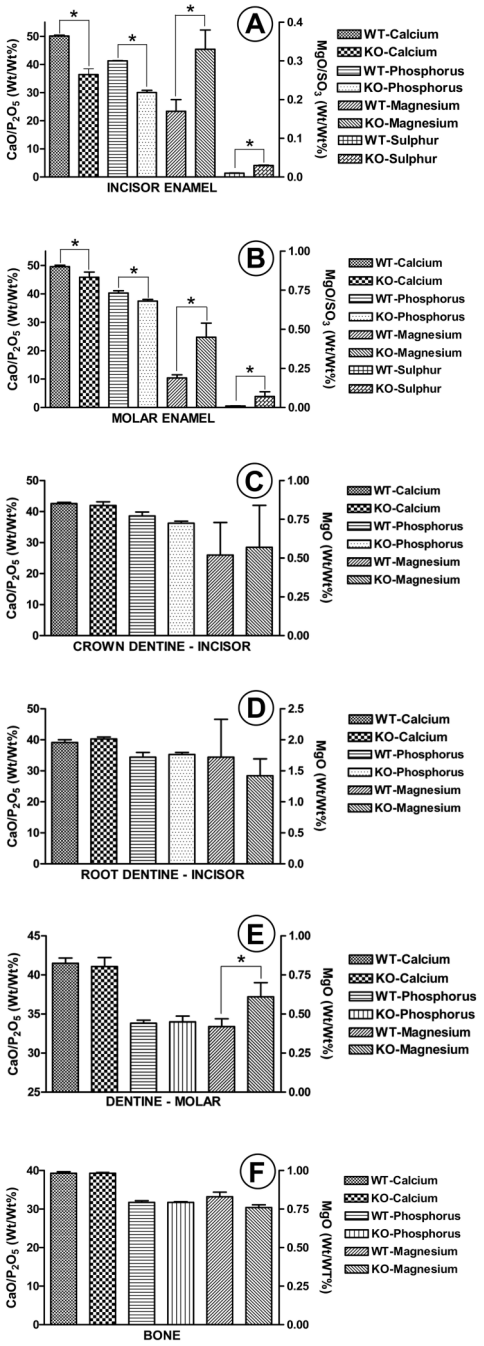

Figure 4A–F.

Figs 4A & 4B show the mineral content in the incisor and molar enamel specimens of $Ae2_{a,b}{}^{+/+}$ (WT) and $Ae2_{a,b}{}^{-/-}$ (KO) animals. All parameters measured were significantly different; i.e., calcium and phosphorus significantly lower and magnesium and sulphur significantly higher in the *Ae2*-deficient mice for both molars and incisors. Figs 4C & 4D show the mineral content of the enamel- and cementum-related incisor dentine. No significant differences could be measured between the $Ae2_{a,b}{}^{+/+}$ (WT) and $Ae2_{a,b}{}^{-/-}$ (KO) specimens in these tissues. Fig. 4E shows the mineral content of molar enamel-related-dentine. The magnesium content was the only parameter that was significantly elevated in the $Ae2_{a,b}{}^{-/-}$ specimens when compared to the $Ae2_{a,b}{}^{+/+}$-specimens. With respect to bone (Fig. 4F), no

significant differences were found between $Ae2_{a,b}^{-/-}$ and $Ae2_{a,b}^{+/+}$ specimens. (* $p<0.01$, X ±SD; n=5 for ($Ae2_{a,b}^{-/-}$ *and n=4 for* $Ae2_{a,b}^{+/+}$).

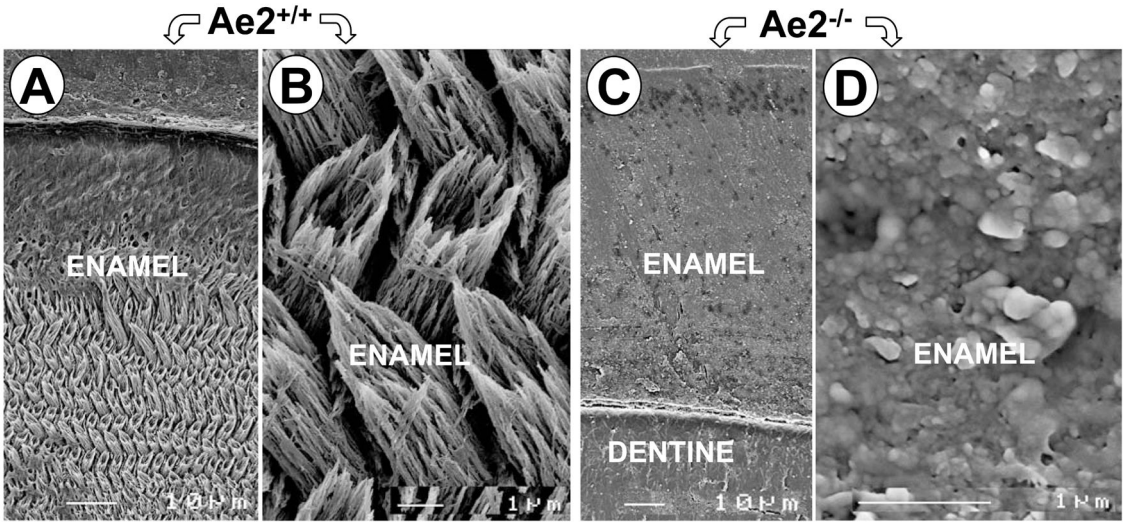

Figure 5A–D.

Scanning electron micrographs of phosphoric acid-etched maturation stage enamel. Figs 5A (survey) and 5B (detail) are of an $Ae2_{a,b}^{+/+}$ specimen. Note the characteristic rod-inter-rod enamel prism structure. Figs 5C and 5D show the corresponding etched enamel structure observed in the $Ae2_{a,b}^{-/-}$ specimens. The rod-inter-rod enamel crystallite structure is completely lost.

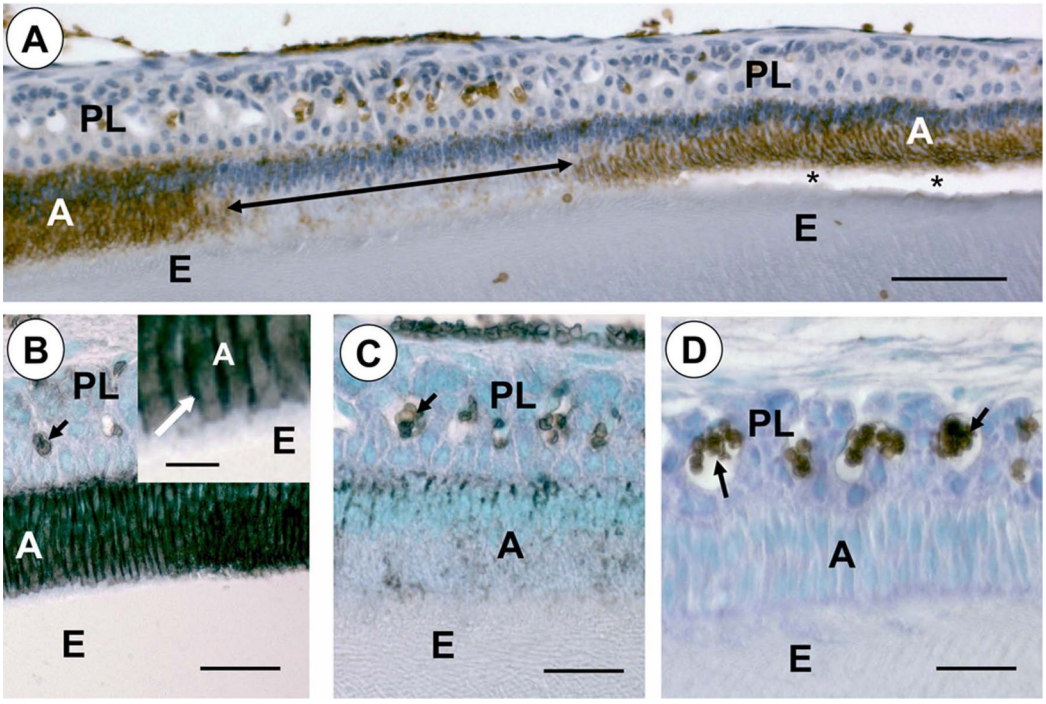

Figure 6A–D.

ABC-peroxidase immuno-staining of Ae2: Intense staining reaction can be seen in the maturation stage ameloblasts (A) of the $Ae2_{a,b}^{+/+}$ specimens (Fig. 6A) but some ameloblast populations were lightly stained (Fig. 6A, double arrow). The reaction product was primarily associated with the lateral plasma membranes of the ameloblasts (white arrow, Fig. 6B, inset). Each specimen always contained a set of contiguous ameloblast cell populations that exhibited very low reaction product (Figs 6A & 6C). The maturation stage ameloblasts of the $Ae2_{a,b}^{-/-}$ specimens were completely negative for the Ae2 peptide reaction product (Fig. 6D). Erythrocytes were intensely stained in the $Ae2_{a,b}^{+/+}$ and the $Ae2_{a,b}^{-/-}$ specimens (arrows, Figs 6B–D) (Bars=50 μm).

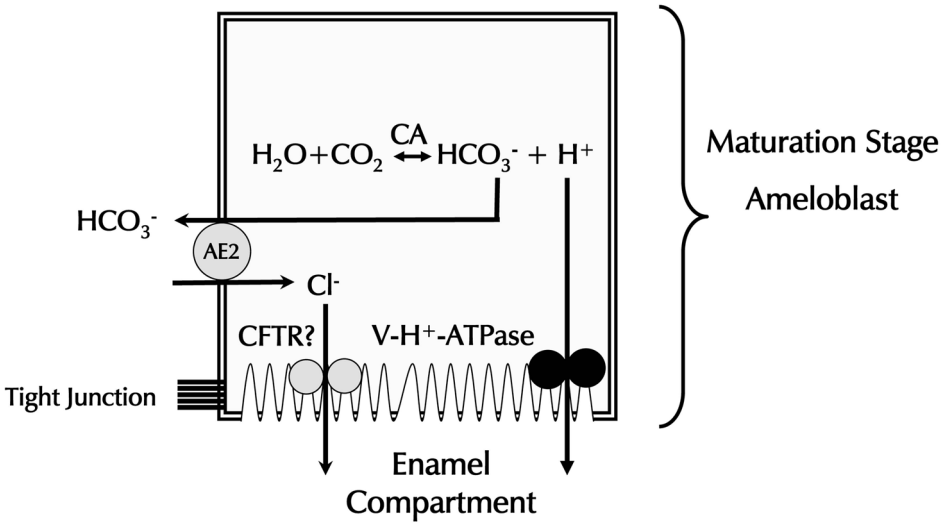

Figure 7.

A model for the function of Ae2 in pH regulation during the maturation stage of amelogenesis in the mouse incisor. This model assumes that the ruffle-ended maturation stage ameloblasts maintain low pH in the enamel layer to catalyse protein hydrolysis and/or to drive the mineralisation process. To maintain this low pH, ameloblasts pump protons, generated by carbonic anhydrase II (CA-II) that is abundantly present in these cells, into the enamel space by the vacuolar H^+-ATPase associated with the ruffle border membrane. The Ae2 associated with the basolateral membranes of the ameloblasts exchanges extracellular Cl^- for intracellular HCO_3^-. The accumulated intracellular Cl^- is probably transported into the enamel compartment by the cystic fibrosis trans-membrane conductance regulator.